Catalysis Today 258 (2015) 602–609

Contents lists available at ScienceDirect

Catalysis Today

journal homepage: www.elsevier.com/locate/cattod

Photocatalytic degradation of three amantadine antiviral drugs as well as their eco-toxicity evolution

Jibin An[a,b], Guiying Li[a], Taicheng An[a,*], Weihua Song[c], Huixia Feng[d], Yujuan Lu[e]

[a] State Key Laboratory of Organic Geochemistry and Guangdong Key Laboratory of Environmental Protection and Resources Utilization, Guangzhou Institute of Geochemistry, Chinese Academy of Sciences, Guangzhou 510640, P. R. China
[b] University of Chinese Academy of Sciences, Beijing 100049, P. R. China
[c] Department of Environmental Science & Engineering, Fudan University, Shanghai 200433, China
[d] College of Petrochemical Technology, Lanzhou University of Technology, Lanzhou 730050, China
[e] Chemistry and Chemical Engineering College, Shenzhen University, Shenzhen 518060, P. R. China

ARTICLE INFO

Article history:
Received 24 October 2014
Received in revised form 12 January 2015
Accepted 14 January 2015
Available online 20 February 2015

Keywords:
Photocatalytic degradation
Antiviral drug
Kinetics
Reactive oxygen species
Ecotoxicity assessment

ABSTRACT

Advanced oxidation processes (AOPs) relying on in situ generated highly reactive •OH are successfully applied to water purification. The absolute reaction rate constants for •OH with three antiviral drugs were first reported through pulsed radiolysis experiments. Results found that •OH reacted quickly with these substrates, with bimolecular reaction rate constants of 6.31×10^9, 5.13×10^9, and 7.05×10^9 $M^{-1}s^{-1}$ for 1-amantadine, 2-amantadine, and rimantadine, respectively. The photocatalytic degradation kinetics of substrates were followed pseudo-first-order kinetics according to Langmuir–Hinshelwood model in TiO_2 suspensions, and the apparent rate constants were obtained as 0.076, 0.084, and 0.102 min^{-1} for three antiviral drugs, respectively. Scavenger experiments revealed that •OH was the major reactive species involved in antiviral drugs degradation. To probe the photocatalytic degradation mechanism, the fate of nitrogen elements and the change of total organic carbon were also examined, and the data showed that all three drugs could be completely mineralized into CO_2, H_2O, and inorganic ions (NO_3^- and NH_4^+) without generating any detectable products with enough degradation time. To further insight into the potential adverse effect of three antiviral drugs and their degradation products, the acute aquatic toxicity of degradation solutions were evaluated at three different trophic levels, and the toxicities first increased slightly and then decreased rapidly as the total organic carbon decreased.

1. Introduction

Pharmaceuticals and personal care products (PPCPs) are emerging organic contaminates (EOCs) that have attracted extensive attention recently due to their occurrence in waters [1,2]. Personal care products are washed directly into the wastewater streams, while a significant portion of pharmaceuticals also enter aquatic environments as both the original forms and metabolized products after use and excretion. Although PPCPs are commonly presented at low concentration (typically ng–μg L^{-1}), they constitute an important concern due to their potential risks to aquatic ecological systems and human health even at trace levels [3–5].

Amantadine and its associated drug, rimantadine, have been approved to protect and treat influenza and Parkinsonism for several decades [6,7]. Both of them are primarily used as therapeutic influenza drugs of people and used as additive drugs for various livestock [8,9]. Both drugs have been widely used in the developing countries, because they are the cheapest ones against flu and affordable drugs. The extensive usage provides a continuous release of them to the water environment, but it is difficult to eliminate these EOCs by traditional wastewater treatment technologies [10,11]. Furthermore, their degradation as well as their potential risk to aquatic ecological systems have never been attempted, although amantadine was known to cause several pharmacologic effects on the central nervous system stimulation at relatively high dose [12].

Advanced oxidation processes (AOPs), based on the production of hydroxyl radical (•OH) as the main oxidative species, can successfully degrade most organic contaminants. Among various AOPs, TiO_2 heterogeneous photocatalysis has been proved to be a promising destructive technology to decontaminate water-soluble refractory pharmaceuticals efficiently and cost-effectively [13,14], due to the process can be carried out under mild condition [15]. The possibilities as well as the mechanisms of the photocatalytic degradation of some pharmaceuticals have been reported [16,17].

* Corresponding author. Tel.: +86 20 85291501; fax: +86 20 85290706.
E-mail address: antc99@gig.ac.cn (T. An).

http://dx.doi.org/10.1016/j.cattod.2015.01.004
0920-5861/

However, most studies were mainly focused on the elimination of parental compounds [17–19], although some degradation products were identified to be more toxicity to the aquatic ecosystems and the public health [20]. Thus, the assessments of possible adverse effects of degradation products on environment are very essential. To our knowledge, the works concerning the photocatalytic decomposition of amantadine and rimantadine in water was never attempted until now. Therefore, their photocatalytic transformation kinetics and mechanism in AOPs, as well as the risk assessment of degradation products are of great concern during the photocatalytic process.

With these backgrounds, the photocatalytic degradation kinetics of three antiviral drugs with the protonation and neutral forms are systematically studied under UV irradiation. In addition, the contribution of different reactive oxygen species to the photocatalytic degradation of substrates is also examined to properly understand its environmental fate and transformation mechanism using different scavengers' addition. Finally, the ecotoxicity risks of three antiviral drugs as well as its degradation products were assessed at three different tropic levels as the total organic carbon decreased slowly.

2. Materials and methods

2.1. Materials

1-Amantadine, 2-amantadine, rimantadine (the structure as shown in Scheme S1) and dansyl chloride (≥99% purity) were purchased from Tokyo Chemical Industry Co., Ltd. Titanium dioxide (TiO_2, P25, Degussa AG, Germany) was used as the photocatalyst. Luminescent bacterium *Ptotobacterium phosphoreum* (*P. phosphoreum*) was purchased from the Institute of Soil Science, Chinese Academy of Sciences (CAS), China. *Selenastrum capricornutum* (*S. capricornutum*) and monoclonal *Daphnia magna* (*D. magna*) were kindly provided by Prof. Xiangping Nie, Institute of Hydrobiology, Jinan University, China. All the solutions were prepared using HPLC grade water, which was obtained by the Milli-Q system by constant illumination with a xenon arc lamp at 172 nm to keep total organic carbon concentration below 13 $\mu g\,L^{-1}$. Methanol and acetonitrile (HPLC grade) obtained from Sigma were used as solvent, and all other chemicals used were of at least analytical-reagent grade.

2.2. Determination of •OH reaction rates

Bimolecular rate constants of •OH reaction with three antiviral drugs were determined using pulse radiolysis with competition kinetic model at Notre Dame Radiation Laboratory (NDRL), with the 8-Mev Titan Beta model TBS-8/16-1S linear accelerator. Dosimetry was performed using N_2O-saturated 0.87 mM KSCN solutions at $\lambda = 472$ nm, with average doses of 3–5 Gy per 2–3 ns pulse. The radiolysis of water is described in Eq. (1), where the numbers in the parentheses are the G-values in $\mu M\,J^{-1}$. All the experimental data were determined by averaging 8–12 replicate pulses using the continuous flow mode of the instrument.

$$H_2O \rightarrow e^-_{aq}[2.7] + {}^{\bullet}H[0.55] + {}^{\bullet}OH[2.7] + H_2[0.45] + H_2O_2[0.71] + H^+[2.7] \quad (1)$$

2.3. Photocatalytic degradation experiments and toxicity assays

The photocatalytic degradation was carried out in an open Pyrex reactor (150 mL, Fig. S1) with a double-walled cooling-water jacket to maintain the constant temperature of the solution ($25 \pm 1\,^{\circ}C$) throughout the experiment. The light source was a high-pressure mercury lamp (GGZ-125, Shanghai Yaming Lighting, $E_{max} = 365$ nm) with a power consumption 125 W, which paralleled to the photocatalytic reactor. The UV light intensity at the surface of the reactor was controlled at 0.36 mW/cm^2, measured with an UV-irradiance meter (UV-A, Beijing Normal University). A 150 mL solution (100 μM) of substrate and certain amount of TiO_2 was added into the reactor according to the experimental designed values. Prior to illumination, the suspension was stirred in the dark for 30 min to achieve the adsorption equilibrium. Then the light was turned on, signaling the start of photocatalysis. At given time intervals, 3 mL treated solution was sampled, and filtered through 0.22 μm Millipore filters to remove TiO_2 particles for further analysis.

The ecotoxicities of treated drug solution were evaluated at three trophic levels: *P. phosphoreum*, *S. capricornutum* and *D. magna*. The detailed procedure can refer to our previous publications [21,22]. For the toxicity bioassay with *P. phosphoreum*, the luminescence was determined with Dxy-3 analyzer (Nanjing Kuake, China), and the toxicity was determined after 15 min incubation. *S. capricornutum* bioassay was carried out according to the Organization for Economic Co-operation and Development (OECD) guideline for alga growth inhibition test No. 201, and the measurement of algal biomass at different exposure times was done by manual cell counting under microscope. *D. magna* bioassay was carried out according to the OECD guideline for *D. magna* acute immobilization test No. 202. The neonates (<24 h hold) of *D. magna* were used in all toxicity assay and 10 animals were used at each treatment in Pyrex beakers containing 50 mL of the test solution. Toxicological endpoint was the immobilization after 24 and 48 h exposure to the treated drug solutions and the definition of immobilization is that daphnia are not able to swim within 15 s after gentle agitation of the test vessel. All the degradation and toxicity assessment experiments were replicated in triplicate.

2.4. Analysis procedure

The analysis of three antiviral drugs was performed with Agilent 1200 series high-performance liquid chromatography (HPLC) equipped with a florescent detector after they were derived with dansyl chloride as shown in Scheme S2. Derivation procedure is shown as follows: The 500 μL dansyl chloride solution was added to 500 μL aliquot of 1-amantadine, 2-amantadine or rimantadine solution and optimized to pH 9.0 as shown in Fig. S2, with sodium bicarbonate–sodium hydroxide buffer solution. The mixture was vortexed and incubated in air bath at 50 °C for 60 min. After the derivation, conditions optimized and shown in Fig. S3, the solution was subjected to HPLC analysis.

HPLC analysis: The concentrations of derivatives were analyzed by Agilent 1200 series HPLC system under the following conditions: Agilent XDB-C18 Eclipse (4.6 × 150, 5 μm particle size) performed at 30 °C. The mobile phases used were water (A) and acetonitrile (B) at flow rate of 1 mL min^{-1}, with the linear gradient elution set as following: 0 min 20% B, 3 min 40% B, 4 min 70% B, 5 min 90% B, 11 min 90% B and 12 min 20% B. The fluorescence detection was setup as excitation at 320 nm and emission at 523 nm.

Ion chromatography (IC): A Dionex ion chromatograph (ICS-900) equipped with a conductivity detector was used for determination of NH_4^+ and NO_3^-. For NH_4^+, the separation was performed on an Ion Pac CS12A (4 × 250 mm, Dionex) column, and 11 mM H_2SO_4 was used as eluent at flow rate of 1.0 mL min^{-1}. For NO_3^-, the separation was performed on an Ion-Pac AS23 anion column (4 × 250 mm, Dionex), and a mixture of sodium carbonate (4.5 mM)/sodium bicarbonate (0.8 mM) was used as eluent at a flow rate of 1.0 mL min^{-1}.

Total organic carbon (TOC): TOC contents of samples were measured with a Shimadzu TOC-5000 analyzer (catalytic oxidation

on Pt at 680 °C). Triplicate analyses were performed for each sample.

3. Results and discussion

3.1. Reaction with •OH

Due to the importance of •OH in both photochemical and photocatalytic degradation of organic process, it is necessary to evaluate the absolute reaction rate constant between organics with •OH. For 1-amantadine, 2-amantadine and rimantadine, their reaction rate constants with •OH were determined using SCN^- competition kinetics based on monitoring the $(SCN)_2^{\bullet-}$ absorption at 472 nm. The reaction of substrates with •OH were shown in Eqs. (2) and (3):

$$\bullet OH + \text{Substrates} \xrightarrow{k_1} H_2O + \text{Substrate}_{\text{intermediate}} \quad (2)$$

$$\bullet OH + 2SCN^- \xrightarrow{k_2} HO^- + (SCN)_2^{\bullet-} \quad (3)$$

Combining these two equations gives the expression

$$\frac{[(SCN)_2^{\bullet-}]_0}{[(SCN)_2^{\bullet-}]} = 1 + \frac{K_1[\text{Substrates}]}{K_2[SCN^-]} \quad (4)$$

where $[(SCN)_2^{\bullet-}]_0$ is the absorbance of this transient at 472 nm when only SCN^- is present and $[(SCN)_2^{\bullet-}]$ is the reduced yield of this transient with increasing concentration of substrates. Therefore, a plot of $[(SCN)_2^{\bullet-}]_0/[(SCN)_2^{\bullet-}]$ against the ratio [Substrates]/[SCN^-] yields a straight line of slope k_1/k_2. With the known rate constant of •OH reaction with SCN^-, $k_2 = 1.1 \times 10^{10}\ M^{-1}\ s^{-1}$, the rate constant ($k_1$) of substrate can be determined.

Fig. 1a shows the transient absorbance intensity of $(SCN)_2^{\bullet-}$ with increasing concentration of 1-amantadine, and a decreased absorbance intensity of $(SCN)_2^{\bullet-}$ was observed with increasing 1-amantadine amounts. Similar patterns of the transient absorbance intensity of $(SCN)_2^{\bullet-}$ were also obtained for other two antiviral drugs as 1-amantadine (figures are not shown). The slope of the transformed plot of Fig. 1a shown in b gives a weighted linear fit corresponding to a reaction rate constant, $6.31 \times 10^9\ M^{-1}\ s^{-1}$, for 1-amantadine, so does 5.13×10^9 and $7.05 \times 10^9\ M^{-1}\ s^{-1}$ for 2-amantadine and rimantadine, respectively. Their reaction rate constants were all at the 10^9 order of magnitude, indicating that •OH was highly reactive to these three antiviral drugs with a diffusion controlled rate [23].

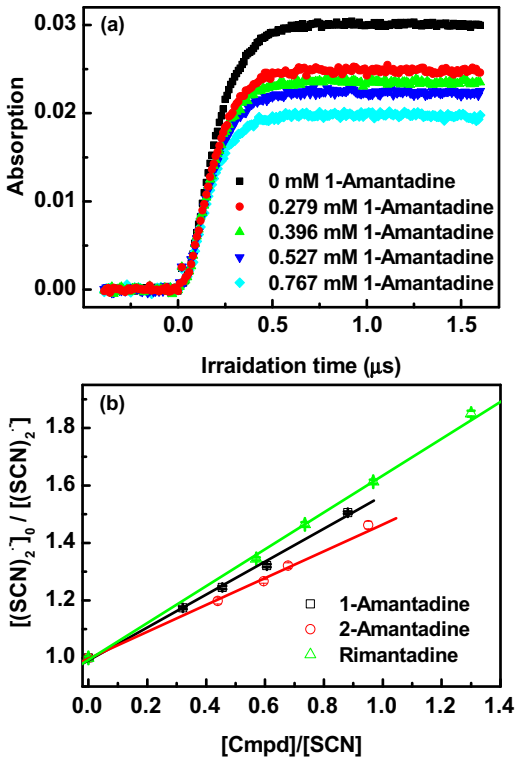

Fig. 1. (a) The formation kinetics of $(SCN)_2^{\bullet-}$ at 472 nm in N_2O saturated 0.87 mM SCN^- containing different concentration of 1-amantadine in phosphate-buffered solutions at pH 7.0 and room temperature; (b) competition kinetic plot for hydroxyl radical reaction with 1-amantadine, 2-amantadine and rimantadine using SCN^- as a standard. The straight line is the weighted linear plots, and the bimolecular reaction rate constants were obtained as 6.31×10^9, 5.13×10^9 and $7.05 \times 10^9\ M^{-1}\ s^{-1}$, respectively.

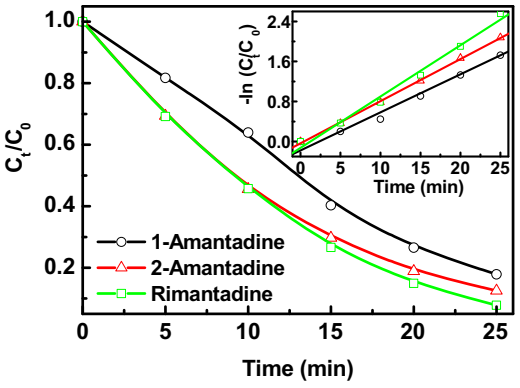

Fig. 2. Photocatalytic degradation of 100 μM 1-amantadine, 2-amantadine and rimantadine with 1.0 g L^{-1} TiO_2. Inset: the linear transformation of $-\ln(C_t/C_0)$ vs. the degradation time, for the disappearances of 1-amantadine, 2-amantadine and rimantadine.

3.2. Degradation kinetics

The photocatalytic degradation of 1-amantadine, 2-amantadine and rimantadine were investigated in TiO_2 suspension solutions, and the preliminary experiments were conducted to evaluate the extent of adsorption and photolysis on the substrates elimination. Figs. S5–S7 show the degradation profiles of 1-amantadine, 2-amantadine and rimantadine (C_t/C_0) under different conditions: (i) in the dark with TiO_2 (adsorption), (ii) UV irradiation without TiO_2 (photolysis) and (iii) UV irradiation with TiO_2 (photocatalysis). As illustrated, the elimination efficiencies of three antiviral drugs by direct photolysis were less than 5% within 2 h, indicating that the direct photochemical degradations are not the key transformation pathways for these three antiviral drugs. Moreover, the removal of them by TiO_2 alone was also insignificant, indicating the negligible adsorption of 1-amantadine, 2-amantadine and rimantadine onto TiO_2 surface. However, in the presence of both TiO_2 with UV light irradiation, nearly 100% substrates were eliminated within 80 min. That is, the adsorption and photolysis play minor role in the photocatalysis degradation of these three drugs.

Numerous studies have implied that the degradation rate of various EOCs by TiO_2 heterogeneous photocatalysis followed the Langmuir–Hinshelwood (L–H) kinetics model [17,24]. When the concentration of organics were very low (mill molar), the L–H kinetic model can be simplified to an apparent-first-order equation $r = k_{app}C_{eq}$ [15], where r is the reaction rate of the substrates and k_{app} is the apparent reaction rate constant. Fig. 2 shows the photocatalytic degradation kinetic profiles of three antiviral drugs in TiO_2 suspension, and the plots of $\ln(C_0/C_t)$ versus the degradation time represent straight line with a good linearity (R^2 value of 0.99, 0.99 and 0.98 for 1-amantadine, 2-amantadine and rimantadine, respectively), indicating that the degradation data were consistent with the L–H model (inset in Fig. 2). The apparent rate constants were calculated as the slope of the regression curves

as 0.076, 0.084 and 0.102 min^{-1} for 1-amantadine, 2-amantadine and rimantadine, respectively. We conclude that amantadine drugs can be degraded quickly in photocatalytic system and rimantadine degraded more quickly than the other two drugs, 1-amantadine, and 2-amantadine.

The acidity or alkalinity of the solution can affect photocatalytic degradation rate of EOCs. It is because pH value can influence the ionization state of TiO_2 surface [25], as well as the yield of the formation of •OH [26,27]. Therefore, the effect of pH value of the solution on the photocatalytic degradation rate of three antiviral drugs was studied. The p*K*a values of three antiviral drugs are 10.8, 10.8 and 10.4 for 1-amantadine, 2-amantadine and rimantadine, respectively [28], suggesting that they generally existed as protonation and neutral forms in water. Thus, the observed apparent rate constants in TiO_2 photocatalysis process were consisted of degradation of protonation and neural form of substrates, as shown in Eqs. (5) and (6):

$$TiO_2/UV + [Substrates]H^+ \xrightarrow{k_1} Products \quad (5)$$

$$TiO_2/UV + [Substrates] \xrightarrow{k_2} Products \quad (6)$$

Therefore, Eq. (7) is derived to calculate the individual rate constant of different existed forms of substrate:

$$k_{app}[Substrate]_{tot} = k_1[Substrate]H^+ + k_2[Substrate] \quad (7)$$

Rearrange Eq. (7) to Eq. (8):

$$k_{app} = \frac{k_1[Substrate]H^+ + k_2[Substrate]}{[Substrate]_{tot}} \quad (8)$$

Thus, Eq. (9) as

$$k_{app} = k_1\sigma_1 + k_2\sigma_2 \quad (9)$$

where $\sigma_1 = [Substrate]H^+/[Substrate]_{tot} = H^+/[K_{a,Cmpd}]$ and $\sigma_2 = [Substrate]/[Substrate]_{tot} = K_{a,Cmpd}/([H^+] + [K_{a,Cmpd}])$ represent the fraction of $[Substrate]H^+$ and [Substrate], respectively, and k_1 and k_2 are the degradation rate constants of the protonation and neutral forms of 1-amantadine, 2-amantadine and rimantadine, respectively. $[Substrate]_{tot}$ is the total concentration of each antiviral drug, $[Substrate]H^+$ is the concentration of protonation forms of 1-amantadine, 2-amantadine and rimantadine, and [Substrate] is the concentration of neutral forms of 1-amantadine, 2-amantadine and rimantadine, respectively. Obviously, $[Substrate]_{tot} = [Substrate]H^+ + [Substrate]$.

Adjusting pH value of solution to 8.6, 9.6, 10.1, 10.6 and 11.1 with sodium hydroxide solution makes the substrates in protonation or neutral form (pH value of 8.6 was chosen as lowest pH value because of three antiviral drugs mainly exist as protonation form at pH <6.8). For 1-amantadine, the species-specific reaction rate constants, k_1 (0.073 min^{-1}) and k_2 (0.101 min^{-1}) were calculated from least-squares nonlinear regressions of the experimental k_{app} data, and the model could describe very well with the experimental k_{app} ($R^2 = 0.91$) (Fig. 3a). Moreover, the photocatalytic degradation of protonation form of 1-amantadine ($k_1\sigma_1$) controls the overall degradation process at pH < 10.4, and the photocatalytic degradation of neutral form of 1-amantadine ($k_1\sigma_1$) controls the overall degradation process at pH > 10.4. As for 2-amantadine, the species-specific reaction rate constants k_1 and k_2 were determined as 0.046 and 0.020 min^{-1}, respectively, and the photocatalytic degradation of protonation or neutral form controls the overall degradation process at pH < 10.8 and pH > 10.8, respectively. While as for rimantadine, k_1 and k_2 were obtained as 0.052 and 0.031 min^{-1}, respectively, and the control of the overall degradation process was at pH 10.4.

As for the speciation of 1-amantadine (Fig. 3a), when pH values increased from 8.6 to 11.1, the protonation form decreased from

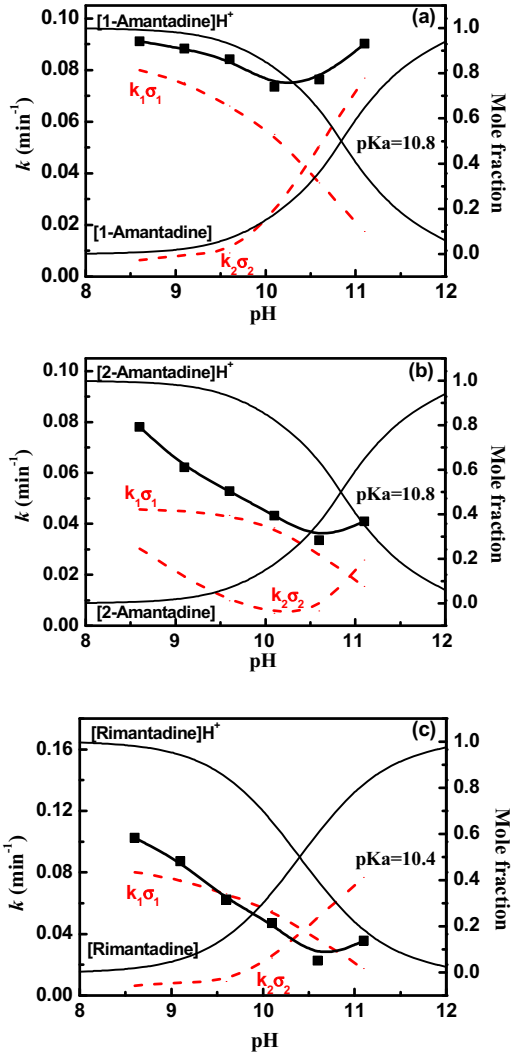

Fig. 3. Effect of pH value on the photocatalytic degradation rate constants of 100 μM 1-amantadine (a), 2-amantadine (b) and rimantadine (c) with 1.0 g L^{-1} TiO_2.

99 to 38%, meanwhile the neutral form increased from 1 to 62%. Thus, the rate constants decreased firstly from 0.091 min^{-1} at pH 8.6 to 0.073 min^{-1} at pH 10.1, and then increased to 0.091 min^{-1} with further increasing pH value up to 11.1. Similar trends of the reaction rate were also observed for 2-amantadine and rimantadine (Fig. 3b and c).

From the above results, it is found that the pH has similar influence on the photocatalytic degradation rate constants of three antiviral drugs. In general, the surface reaction is a rate-determining step for the photocatalysis, thus the photocatalytic degradation of organics was strongly depended on the association between the surface of catalyst and substrates [16,29]. That is, the photocatalytic degradation occurred mainly on the surface of TiO_2 by the oxidation reactions with photoholes or •OH [30]. The point of zero charge of TiO_2 is at pH 6.3. That is, TiO_2 surface is negatively charged in all investigated solution. Meanwhile, when pH value increased from 8.6 to p*K*a value of substrates, the protonation form of substrates gradually decreased, and the neutral form of substrates gradually increased, resulting in a decreased electrostatic adsorption between the substrates and catalyst surface. Therefore, the electrostatic repulsion retards their contact and subsequently results in reducing photocatalytic degradation rate. Furthermore, the increase in degradation rate was observed with increasing pH

value, which is mainly due to that •OH can be easily generated in alkaline solution, and •OH was considered as the predominant species at high pH value [31]. Overall, although it is a daunting work to interpret the pH effect on the photocatalytic degradation of various organics due to the multiple roles of pH value, we can confirm that the form of substrates control overall photocatalytic degradation process by calculation of the reaction rate of different forms of substrates.

3.3. The contribution of different reactive spices and the degradation mechanism

Isopropanol and potassium iodide (KI) were often used as scavengers to capture reactive oxygen species during the photocatalytic reaction. Isopropanol is considered as a •OH scavenger with a reaction rate constant (k) of $1.9 \times 10^9\ M^{-1}\ s^{-1}$ to discriminate the role between the h^+ and •OH [24]. Different concentrations of isopropanol were added to evaluate the effect on photocatalytic degradation of three antiviral drugs (Fig. 4). Dividing the reaction rates of isopropanol from substrates with •OH, Eq. (10) was deduced:

$$r_{ISO} = \frac{r_{0,ISO}}{r_{0,substrate}} = \frac{k_{0,ISO}C_{\bullet OH}C_{0,ISO}}{k_{0,substrate}C_{\bullet OH}C_{0,substrate}} = 0.26\frac{C_{0,ISO}}{C_{0,substrate}} = 0.26\alpha_{ISO} \quad (10)$$

where r_{ISO} is the ratio of the reaction rate of isopropanol to substrates with •OH and α_{ISO} is the ratio of isopropanol over substrates concentration.

By adjusting the concentration ratio of isopropanol to substrates results in an r_{ISO} from 0.26 to 260, and an obvious decrease in degradation rate constant was noticed for all three antiviral drugs. Such as at $\alpha_{ISO} = 100$, the initial degradation rate of isopropanol with •OH was 26 times higher than that of substrate alone. For instance, the drop of 83.2, 88.2 and 76.6% in the degradation rate constants were observed for 1-amantadine, 2-amantadine and rimantadine, respectively (Table 1). And when $\alpha_{ISO} = 1000$, the drop of 100% in the degradation rate constants were observed for all investigated drugs. It is concluded that •OH is an important contributor to the photocatalytic degradation of these three antiviral drugs.

In addition, the iodide ion is used to evaluate the contribution of both valence h^+ and •OH [32]. As different concentrations of KI were added during the photocatalytic degradation of 1-amantadine, 2-amantadine and rimantadine (Fig. 4), an obvious decrease in degradation rate constant was observed. At $\alpha_{KI} = 100$, a decrease of 94.84, 98.13 and 88.52% in the degradation rate constant was observed for three drugs, respectively (Table 1). When applying KI concentrations at $\alpha_{KI} = 1000$, a decrease of 100% in the degradation rate constant was also observed for substrates due to complete quenching of h^+ and •OH. Moreover, the percentage of contribution of •OH were 2–19 times higher than that of

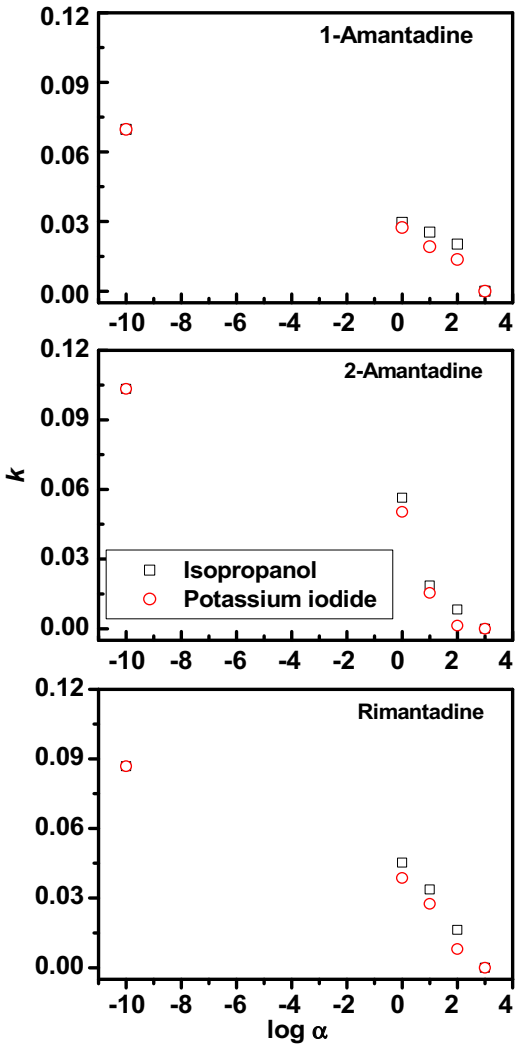

Fig. 4. Photocatalytic degradation rate constant of 1-amantadine, 2-amantadine and rimantadine as function of different isopropanol and potassium iodide concentration expressed as the ratio of α.

Table 1
Percentage of inhibition efficiencies due to the scavengers ISO and KI, and percentage of contribution of •OH and h^+ during the photocatalytic degradation of 1-amantadine, 2-amantadine and rimantadine.

	α_{ISO}	α_{KI}	Percentage of inhibition		Percentage of contribution	
			ISO (%)	KI (%)	•OH (%)	h^+ (%)
1-Amantadine	1	1	57.53	60.69	57.53	3.16
	10	10	73.57	84.07	73.57	10.5
	100	100	83.16	94.84	83.16	11.68
	1000	1000	100	100	–	–
2-Amantadine	1	1	19.08	27.83	19.08	8.75
	10	10	73.31	77.91	73.31	4.59
	100	100	88.24	98.13	88.24	9.89
	1000	1000	100	100	–	–
Rimantadine	1	1	35.01	44.48	35.01	9.47
	10	10	73.65	82.07	73.65	8.42
	100	100	76.61	88.52	76.61	11.91
	1000	1000	100	100	–	–

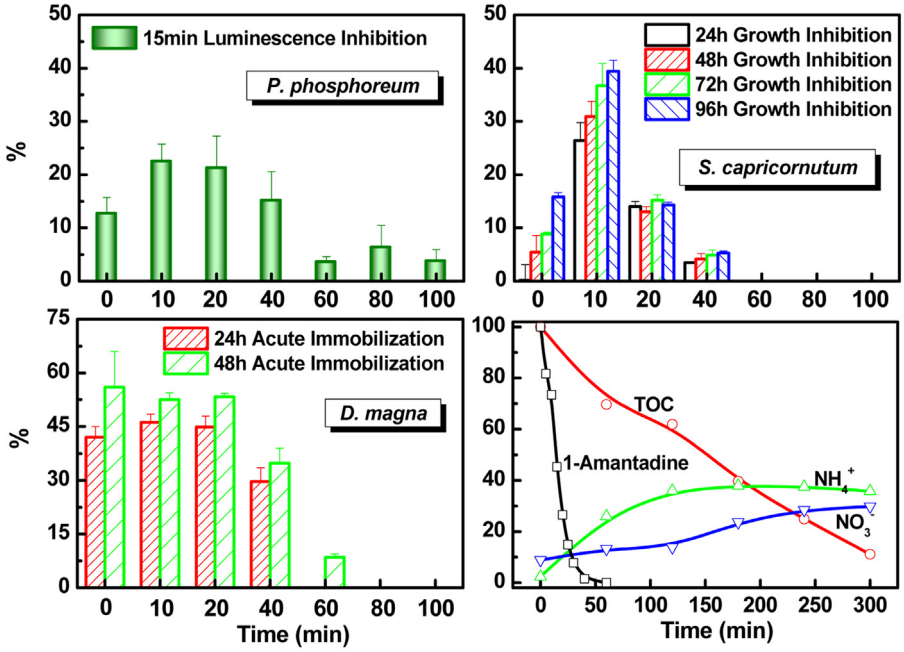

Fig. 5. Evaluation of acute toxicity of 1-amantadine solution with *P. phosphoreum*, *S. capricornutum* and *D. magna* during the treatment.

photogenerated h^+, indicating that h^+ just plays a minor role in the photocatalytic degradation of these three drugs.

In summary, the strongest oxidants, •OH played an important role but h^+ just played a minor role in the degradation of these three antiviral drugs. In photocatalytic system, these EOCs can be efficiently degraded by •OH unselectively into many small inorganic molecules. Experiments on the identification of degradation products were therefore carried out to insight into the photocatalytic degradation mechanism of this kind EOCs. However, no degradation product was observed and identified due to high noise-to-signal ratio although Agilent iron-trap mass spectrometer (MSD-Trap-XTC) was used to trap their intermediates (Fig. S8). Thus, to further evaluate transformation fate of three antiviral drugs and the complete mineralization of the intermediates during AOPs, the evolution of TOC as well as nitrogen element were also measured during the photocatalytic degradation (Figs. 5–7). After 300 min irradiation, only 11.3, 9.2 and 8.3% of TOC were remained for 1-amantadine, 2-amantadine and rimantadine, respectively. That is, almost all three antiviral drugs can be completely decontaminated with the mineralization efficiencies of 88.7, 90.8 and 91.7% accorded with the trendies of degradation rate. At the same time, around 35.8, 29.9 and 38.7% of the nitrogen element were released as NH_4^+ ions, while 34.1, 44.2 and 32.8% were oxidized to NO_3^- ions for 1-amantadine, 2-amantadine and rimantadine, respectively. These results indicated that three antiviral drugs could be easily degraded, and the intermediates could be quickly transformed and finally mineralized into CO_2, water and inorganic ions by various AOPs such as TiO_2 heterogeneous photocatalysis.

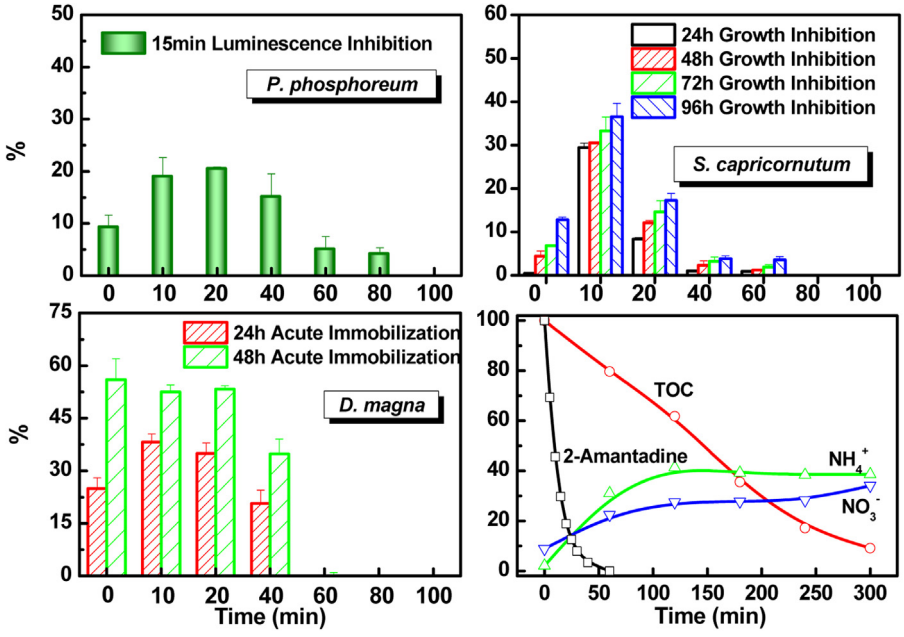

Fig. 6. Evaluation of acute toxicity of 2-amantadine solutions with *P. phosphoreum*, *S. capricornutum* and *D. magna* during the treatment.

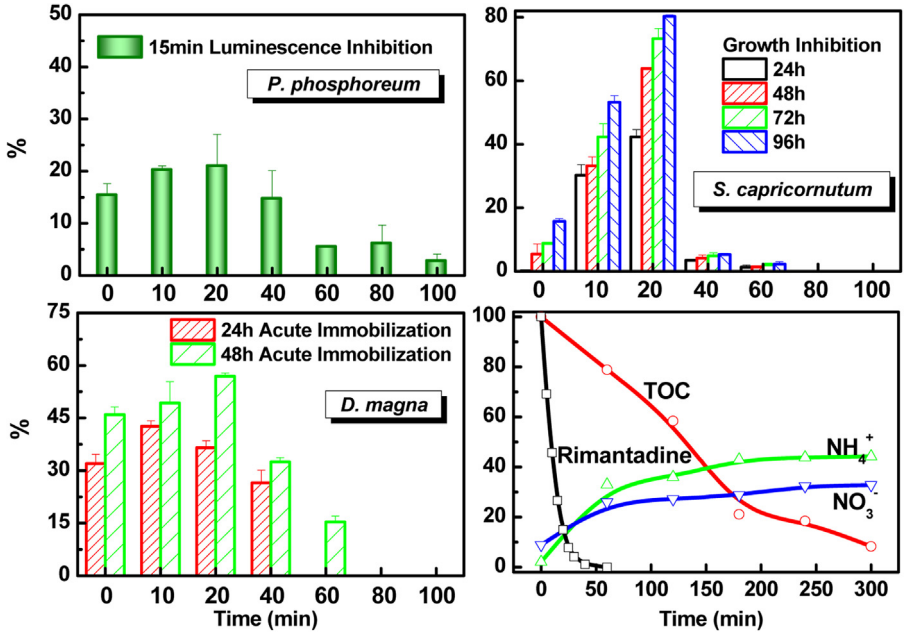

Fig. 7. Evaluation of acute toxicity of rimantadine solutions with *P. phosphoreum*, *S. capricornutum* and *D. magna* during the treatment.

3.4. Ecotoxicity evolution of treated solution

To further confirm the decontamination of these antiviral drugs and investigate the potential risk of their degradation products during the photocatalytic degradation process, the ecotoxicity evolution was evaluated at three different tropic levels, *P. phosphoreum*, *S. capricornutum* and *D. magna*. As shown in Figs. 5–7, *P. phosphoreum* (15 min), *S. capricornutum* (72 h) and *D. magna* (48 h) were found to be inhibited by 12.6, 8.9 and 56.0% for 0.1 mM 1-amantadine, 9.8, 6.9 and 56.0% for 0.1 mM 2-amantadine, and 15.4, 8.9 and 46.0% for 0.1 mM rimantadine exposure, respectively. As degradation processed, the residual concentration of three drugs decreased rapidly, and the increase in the ecotoxicity of treated solutions toward three level species were also observed at initial stage. When almost 85% of substrates were eliminated within 20 min, the inhibition efficiencies of treated solution to *P. phosphoreum*, *S. capricornutum* and *D. magna* remained at 21.2, 15.2 and 53.3% for 1-amantadine, 20.5, 14.6 and 53.3% for 2-amantadine and 21.0, 73.2 and 56.9% for rimantadine, respectively. It implies that the higher toxic intermediates were produced, or somehow synergistic effect existed between the degradation products. However, with further extension of the degradation time, the substrates and products could be mineralized and the acute toxicity of treated solutions decreased significantly as TOC was reduced. For instance, the inhibition efficiencies of treated solutions to *S. capricornutum* and *D. magna* decreased gradually and finally disappeared completely from 20 to 80 min, although the final treated solutions still have a weak inhibition effect on *P. phosphoreum* (6.3, 4.1 and 6.1% for 1-amantadine, 2-amantadine and rimantadine, respectively). Overall, the photocatalytic degradation of these three antiviral drugs can be accomplished successfully. But, as for detoxification of them, sufficient time should be provided for complete decomposing of the products to CO_2 and H_2O. That is, the treatment duration of AOPs should be determined carefully for the safety of ecological environment.

4. Conclusions

The photocatalytic degradation of three antiviral drugs, 1-amantadine, 2-amantadine and rimantadine, were investigated in water environment. It is clear that the adsorption and photolysis were insignificant in the photocatalytic elimination of substrates, while nearly 100% of substrates were eliminated within 80 min in photocatalytic process. Solution pH significantly influences the electrostatic adsorption between the protonation form of substrates and catalyst surface, and subsequently affects the degradation rate of substrates. Further study on the contribution of ROSs indicates that $^{\bullet}OH$ is dominantly responsible for the degradation of three antiviral drugs, while the photogenerated holes just play a minor role in this process. All three investigated antiviral drugs could be completely mineralized with enough irradiation time, and the ecotoxicity assessment of photocatalytic-treated solutions shown that the acute toxicity at three tropic levels of these antiviral drugs can be accomplished by TiO_2 photocatalytic process. Therefore, AOPs, for example, TiO_2 photocatalysis can be further confirmed again as a promising technology to detoxify EOCs, for example, PPCPs.

Acknowledgments

This is contribution No. IS-2016 from GIGCAS. The authors appreciate the financial support from the National Natural Science Funds for Distinguished Young Scholars (41425015), Knowledge Innovation Program of CAS (KZCX2-YW-QN103), Science and Technology Project of Guangdong Province, China (2012A032300010), Open project of SKLOG (OGL-201105) and Earmarked Fund of SKLOG (SKLOG2011A02).

Appendix A. Supplementary data

Supplementary data associated with this article can be found, in the online version, at http://dx.doi.org/10.1016/j.cattod.2015.01.004.

References

[1] D. Fatta-Kassinos, M.I. Vasquez, K. Kümmerer, Chemosphere 85 (2011) 693–709.
[2] C. Prasse, M.P. Schlusener, R. Schulz, T.A. Ternes, Environ. Sci. Technol. 44 (2010) 1728–1735.
[3] S.K. Khetan, T.J. Collins, Chem. Rev. 107 (2007) 2319–2364.

[4] R.P. Schwarzenbach, B.I. Escher, K. Fenner, T.B. Hofstetter, C.A. Johnson, U. von Gunten, B. Wehrli, Science 313 (2006) 1072–1077.
[5] C.G. Daughton, T.A. Ternes, Environ. Health Perspect. 107 (1999) 907–938.
[6] A.A. Smorodintsev, D.M. Zlydnikov, A.M. Kiseleva, J.A. Romanov, A.P. Kazantsev, V.I. Rumovsky, J. Am. Med. Assoc. 213 (1970) 1448–1454.
[7] G.C. Ghosh, N. Nakada, N. Yamashita, H. Tanaka, Chemosphere 81 (2010) 13–17.
[8] G. He, J. Qiao, C. Dong, C. He, L. Zhao, Y. Tian, Antiviral Res. 77 (2008) 72–76.
[9] D. Cyranoski, Nature 435 (2005) 1009.
[10] A. Jelic, M. Gros, A. Ginebreda, R. Cespedes-Sanchez, F. Ventura, M. Petrovic, D. Barcelo, Water Res. 45 (2011) 1165–1176.
[11] L.H. Gao, Y.L. Shi, W.H. Li, H.Y. Niu, J.M. Liu, Y.Q. Cai, Chemosphere 86 (2012) 665–671.
[12] V.G. Vernier, J.B. Harmon, J.M. Stump, T.E. Lynes, J.P. Marvel, D.H. Smith, Toxicol. Appl. Pharmacol. 15 (1969) 642–665.
[13] T.C. An, H. Yang, W.H. Song, G.Y. Li, H.Y. Luo, W.J. Cooper, J. Phys. Chem. A 114 (2010) 2569–2575.
[14] M. Klavarioti, D. Mantzavinos, D. Kassinos, Environ. Int. 35 (2009) 402–417.
[15] H. Yang, G.Y. Li, T.C. An, Y.P. Gao, J.M. Fu, Catal. Today 153 (2010) 200–207.
[16] T.C. An, J.B. An, H. Yang, G.Y. Li, H.X. Feng, X.P. Nie, J. Hazard. Mater. 197 (2011) 229–236.
[17] S. Yurdakal, V. Loddo, V. Augugliaro, H. Berber, G. Palmisano, L. Palmisano, Catal. Today 129 (2007) 9–15.
[18] R.A. Palominos, M.A. Mondaca, A. Giraldo, G. Peñuela, M. Pérez-Moya, H.D. Mansilla, Catal. Today 144 (2009) 100–105.
[19] L. Yang, L.E. Yu, M.B. Ray, Water Res. 42 (2008) 3480–3488.
[20] D. Vogna, R. Marotta, R. Andreozzi, A. Napolitano, M. d'Ischia, Chemosphere 54 (2004) 497–505.
[21] H.S. Fang, Y.P. Gao, G.Y. Li, J.B. An, P.K. Wong, H.Y. Fu, S.D. Yao, X.P. Nie, T.C. An, Environ. Sci. Technol. 47 (2013) 2704–2712.
[22] T.C. An, J.B. An, Y.P. Gao, G.Y. Li, H.S. Fang, W.H. Song, Appl. Catal. B 164 (2015) 279–287.
[23] T.C. An, H. Yang, G.Y. Li, W.H. Song, W.J. Cooper, X.P. Nie, Appl. Catal. B 94 (2010) 288–294.
[24] A. Amine-Khodja, A. Boulkamh, C. Richard, Appl. Catal. B 59 (2005) 147–154.
[25] D.H. Kim, M.A. Anderson, J. Photochem. Photobiol. A: Chem. 94 (1996) 221–229.
[26] C. Galindo, P. Jacques, A. Kalt, J. Photochem. Photobiol. A: Chem. 130 (2000) 35–47.
[27] Z. Shourong, H. Qingguo, Z. Jun, W. Bingkun, J. Photochem. Photobiol. A: Chem. 108 (1997) 235–238.
[28] A.A. Holazo, N. Choma, S.Y. Brown, L.F. Lee, R.J. Wills, Antimicrob. Agents Chemother. 33 (1989) 820–823.
[29] T.C. An, Y. Xiong, G.Y. Li, C.H. Zha, X.H. Zhu, J. Photochem. Photobiol. A: Chem. 152 (2002) 155–165.
[30] H. Yang, T.C. An, G.Y. Li, W.H. Song, W.J. Cooper, H.Y. Luo, X.D. Guo, J. Hazard. Mater. 179 (2010) 834–839.
[31] W.Z. Tang, C.P. Huang, Water Res. 29 (1995) 745–756.
[32] J. Rabani, K. Yamashita, K. Ushida, J. Stark, A. Kira, J. Phys. Chem. B 102 (1998) 1689–1695.